Journal of Applied Polymer Science

Exceptional enhancement of ductility and toughness in poly(vinylidene fluoride)/carbon nanotubes composites

Xuelong Chen,[1] Yen Nan Liang,[1] Ming Yin,[1] Sunanda Roy,[1] Gad Marom,[2] Yongfeng Men,[3] Xiao Hu[1]

[1]School of Material Science and Engineering, Nanyang Technological University, Nanyang Avenue, Singapore 639798, Singapore
[2]Casali Institute of Applied Chemistry, the Institute of Chemistry, the Hebrew University of Jerusalem, Jerusalem, 91904, Israel
[3]State Key Laboratory of Polymer Physics and Chemistry, Changchun Institute of Applied Chemistry, Chinese Academy of Sciences, University of Chinese Academy of Sciences, Changchun 130022, People's Republic of China
Correspondence to: X. Hu (E-mail: ASXHU@ntu.edu.sg)

ABSTRACT: The reinforcement of mechanical properties of polymeric materials is often important for widening their applications; however, it remains a technical challenge to effectively increase toughness without degrading stiffness and strength of the polymers. In this work, by a facile methodology combining solution mixing and melt blending, poly(vinylidene fluoride)/multi-walled carbon nanotubes (PVDF/MWCNTs) composite with exceptionally enhanced ductility and toughness are prepared. With only 0.2 wt % CNT loading, the elongation at break has increased from originally 138% to almost 500%, while toughness improved by as much as 386%, without compromising the stiffness and strength. Note that raw CNTs are directly dispersed in the matrix without any surface modification. In order to elucidate this novel enhancement of ductility of PVDF/MWCNTs composites, we carried out detailed analyses based on results from ultra-small-angle X-ray scattering (USAXS), cryo-fractured surface morphology, differential scanning calorimetry (DSC), and Fourier transform infrared spectroscopy (FTIR). It is proposed that the enhanced ductility are contributed by a synergistic combination of "void pinning effect" of CNT, as well as the formation of γ phase polymorph as the interphase in the PVDF/CNTs composites. © 2016 Wiley Periodicals, Inc. J. Appl. Polym. Sci. **2016**, *133*, 43610.

KEYWORDS: composites; graphene and fullerenes; mechanical properties; nanotubes; phase behavior; polyamides; properties and characterization; structure-property relations; thermal properties

Received 7 January 2016; accepted 6 March 2016
DOI: 10.1002/app.43610

INTRODUCTION

Polymer-matrix composites, synergistically combining the advantages of both polymers and fillers, have found applications in structural reinforcement, electronics, optoelectronics, and many other areas.[1–3] Poly (vinylidene fluoride) (PVDF) has received much research attention in the past few years for its unique piezoelectric and pyroelectric properties.[4,5] Owing to its excellent mechanical properties as well as thermal and chemical stability, PVDF has also been utilized as structural material in architectural, automotive, and chemical processing industry.[6–8] In view of the widening applications of PVDF, it is highly desirable to improve its mechanical properties by employing facile and scalable methods. Carbon nanotube (CNT), contributed by its excellent functional and mechanical properties, represents one of the nano-fillers that has been extensively explored for reinforcement of both thermoplastic and thermoset polymer matrices.[9]

There are several previous studies that used CNTs to reinforce PVDF for preparing high performance composite materials.[10–13] Usually, the introduction of CNT increases modulus and tensile strength of PVDF composite at the cost of reducing the elongation at break. For instance, Amit *et al.* reported PVDF composites reinforced with MWCNTs (functionalized by methyl methacrylate) via a solution casting method.[10] The modulus and tensile strength of the PVDF/MWCNTs composites progressively increased with the increase of CNT loading to 5.0 wt %, with the elongation at break decreased by about 30%. Huang *et al.*[11] prepared PVDF/MWCNTs composites with 0.1 wt % CNT, achieving an increase of modulus (from 1.46 to 1.61 GPa) and tensile strength (from 4.2 to 4.5 MPa); however, with a decrease of elongation at break from 8.5 to 7.3%. In another study conducted by Tang *et al.*,[12] the prepared composite with 0.5 wt % CNT loading in PVDF gained a slight enhancement in modulus and tensile strength, but the elongation at break decreased severely from 250% of neat PVDF to around only 30%. Even when metal particles were deposited onto the surface of CNT, which is claimed to be able to remarkably improve the

Additional Supporting Information may be found in the online version of this article.

ductility, the elongation at break could not match that of neat PVDF.[12] Besides PVDF, the compromise between strength/modulus and ductility is frequently observed in various other polymer/CNTs systems, such as polystyrene, polyethylene, polypropylene, poly(methyl methacrylate), polycarbonate, poly(vinyl alcohol), polyacrylonitrile, polyamide, polyurethane, and epoxy.[14–16]

Interestingly, counterintuitive results have also been documented in the system of CNT strengthened PVDF. Chang *et al.*[13] reported PVDF/MWCNTs composites with largely decreased tensile strength and Young's modulus with 3 wt % CNTs, but with an increased elongation at break from 3.6 to 7.9%, compared with that of neat PVDF. The discrepancy among these works is partially due to different composites fabrication procedures as well as poor interfacial wetting between the fillers and highly fluorinated matrix. On the other hand, the polymorphic transformation in PVDF caused by fabrication techniques also plays important roles. Most of the previous works on PVDF/CNTs composites required tedious surface functionalization of the CNTs; and limited enhancement of mechanical properties were achieved at the expense of decreased ductility. Furthermore, there is very limited discussion across the literature on the effect of polymorphism toward performance of PVDF/MWCNT composites.

In this study, we report the fabrication of highly ductile PVDF/MWCNT composites prepared via a facile method combining solution mixing and melt extrusion. Excellent dispersion of raw MWCNTs in PVDF was achieved without the need of any surface functionalization of CNTs. Contrary to the usual cases; in our work, substantial enhancement in ductility by 400% in the PVDF/MWCNT composites with little change of modulus and yield strength were achieved. Seeing the counterintuitive enhancement of ductility observed in these PVDF/MWCNT composites, we carried out investigation on contributing mechanisms by characterizing systematically the void formation, interphase formation, phase transition during deformation, as well as filler-induced PVDF crystal polymorphism during deformation with and without the presence of MWCNTs.

EXPERIMENTAL

Materials

Poly(vinylidene fluoride) (PVDF) in powder form was purchased from Alfa Aesar and multi-walled carbon nanotubes (MWCNTs) with average diameter of 10 nm and average length of 1.5 μm was purchased from Nanocyl, Belgium. PVDF and CNTs were dried at 100 °C inside vacuum oven overnight before usage. Analytical grade acetone is supplied by Merck and used as received.

Sample Preparation

The procedure to fabricate PVDF/CNTs composites is as follows. First, CNTs with calculated weight percentages (0, 0.1, 0.2, 0.5, and 1.0 wt %) were processed with probe sonication (ultrasonic processor VCX 130, SONICS) in 50 mL acetone for 5 min, with cooling inside ice-water bath. After that, dissolved PVDF in 50 mL acetone was mixed with CNTs solution by magnetic stirring for 1 h before bath sonication for 2 h. The uniform PVDF/CNTs/acetone solution was subjected to solvent evaporation at room temperature, followed by drying inside vacuum oven at 60 °C overnight to completely remove the residual solvent. The products obtained were further extruded by a mini-extruder (HAAKE MiniLab) at 190 °C, 80 rad/minute for 10 min. The obtained composites were finally pressed into thin films with thickness around 0.2 mm by hot-press at 240 °C, and they were used for further characterizations.

Characterization

The morphology of cryo-fractured surfaces of as-prepared samples was studied by field emission scanning electron microscope (FESEM) (JEOL JSM-7600F). Cryo-fractured samples were prepared by fracturing after immersing in liquid nitrogen, before coated with a thin layer of platinum for observation. Mechanical properties were tested with Microtester Instron 5848. Attenuated total reflectance -Fourier transform infrared spectroscopy (ATR-FTIR) spectra were recorded by Perkin Elmer Frontier FT-NIR/MIR spectrometers, with resolution of 2 cm^{-1} for 16 scans. X-ray diffraction (XRD) was performed by a Bruker AXS D8 advance X-ray diffractometer with a Cu Kα X-ray source. Differential scanning calorimetry (DSC) (TA Instruments 2010) was performed from room temperature to 200 °C with a heating rate of 10 °C/min. In situ ultra-small-angle X-ray scattering (USAXS) experiments were carried out by a modified Xeuss system of XENOCS with a semiconductor detector (Pilatus 100K, DECTRIS, Swiss) attached to a multilayer focused Cu Kα X-ray source (GeniX3D Cu ULD, Xenocs SA, France), generated at 50 kV and 0.6 mA. The beam was collimated with a two scatterless slits systems mounted 2.4 meters away from each other. The distance between the sample and detector is 6450 mm, with exposure time of 600 s and beam size of 0.6 $\times$ 0.6 mm^2.

RESULTS AND DISCUSSION

Prior to the testing of the composites, CNTs dispersion inside PVDF was analyzed by examining the morphology of the cryo-fractured surfaces of PVDF/CNTs composites using FESEM, the images are shown in Figure 1. Overall, uniform dispersion of raw CNTs was achieved in all samples prepared by our method. Such excellent dispersion of untreated MWCNT in a polymer matrix is rarely seen in literature. The internal morphology of the composites is important because it directly determines the mechanical and many other physical properties. Aggregation of CNTs could severely deteriorate the mechanical performance of final products due to undesirable localized stress concentration. In our preliminary study, severe aggregation was also observed in samples prepared by only melt blending using the twin-screw extruder (Supporting Information Figure S1a,b); while solution blending gave individually separated CNTs, their distribution was poor, i.e., not uniform throughout the matrix (see Supporting Information Figure S1c,d).

Table I shows the mechanical data obtained from tensile test of neat PVDF and its CNTs composites. It is seen that, for the modulus, there is a slight initial decrease followed by an increase after the introduction of CNTs into PVDF. The yield stresses of all composite samples are marginally lower than that of the neat polymer. Interestingly, the elongation at break has increased to 411, 483, and 361% for samples with 0.1, 0.2, and

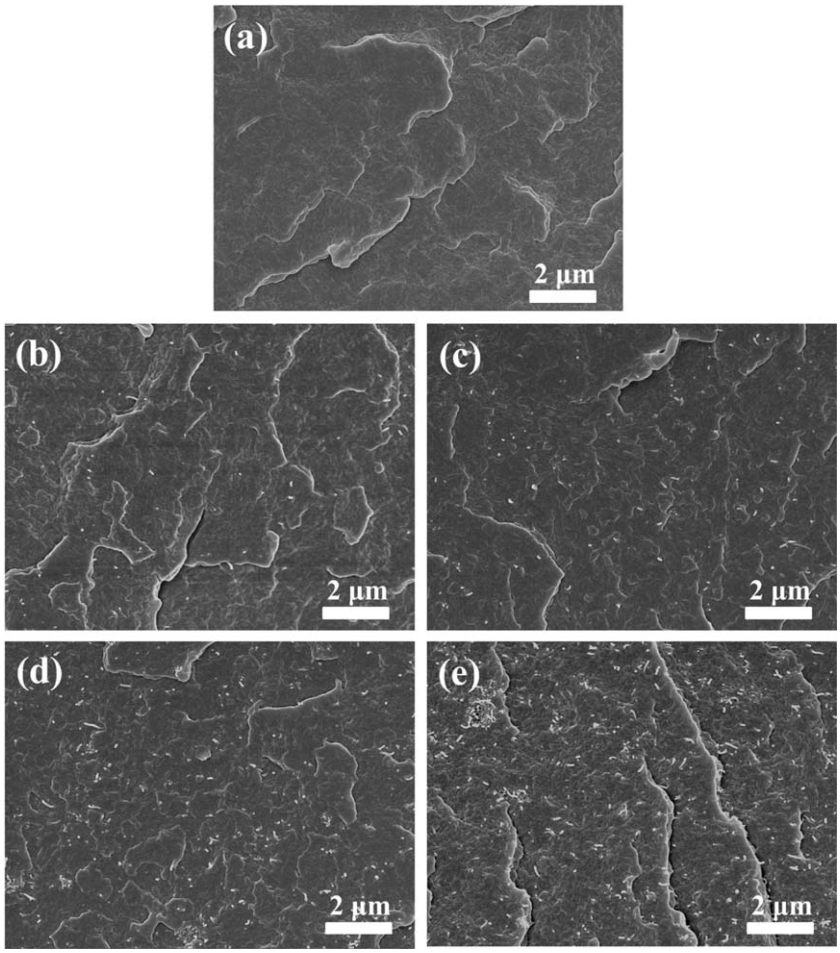

Figure 1. FESEM images of the cyro-fractured surface of (a) raw PVDF and PVDF/MWCNTs composites with CNTs loading of (b) 0.1 (c) 0.2 (d) 0.5 and (e) 1.0 wt %, respectively.

0.5 wt % CNT, as compared with that of neat polymer. Such substantial improvement of ductility without compromise in modulus and strength has never been reported previously in CNTs reinforced polymers.

Figure 2(a) shows representative stress−strain curves of neat PVDF and composite with 0.2 wt % CNT content. The elongation at break of neat PVDF is 128%, while that of the composite sample increased to 483%. The peak in the stress−strain curve around 230% is due to non-equilibrium necking during the stretching process. As a result of greatly increased ductility and comparable modulus and strength, the toughness of the composite samples (defined as the area under stress−strain curve) has significantly increased. The bar diagram in Figure 2(b) shows the toughness increments of all CNTs composites as compared with that of neat PVDF; the normalized increment of tensile toughness of composite with CNT loading of 0.1, 0.2, and 0.5 wt % are 291, 386, and 298%, respectively. With as low as only 0.2 wt % pristine CNTs, the tensile toughness almost quadrupled. This is nontrivial and exceptional, requiring further research effort to investigate the underlying mechanism. Nevertheless, with further increase of CNTs up to 1.0 wt %, toughness decreased due to the poorer dispersion of CNT at higher loading that leads to decreased elongation at break.

Table I. Summarized Mechanical Data of PVDF/CNTs Composites

CNT content (wt %)	Young's Modulus (MPa)	Yield stress (MPa)	Elongation at break (%)
0	504 (15)[a]	47.5 (1.0)	128 (81)
0.1	457 (38)	46.0 (1.7)	411 (89)
0.2	491 (23)	45.8 (0.8)	483 (24)
0.5	532 (17)	46.6 (0.3)	361 (101)
1.0	551 (24)	47.3 (1.0)	113 (85)

[a] Values in parenthesis are the standard deviation. At least five samples for each composite condition were tested.

The reinforcement effect of CNTs on polymer modulus/strength is widely reported and discussed. However, CNTs induced improvement of ductility is very rare in the literature. The understanding of the mechanism behind the enhanced ductility is highly desirable for both academic interests and practical applications. It is well accepted that plasticizer or debonding/cavitation can both contribute to increased ductility.[17−19] The plasticizer effect may originate from solvent, moisture, or low molecular weight additives. In our work, since the fabrication

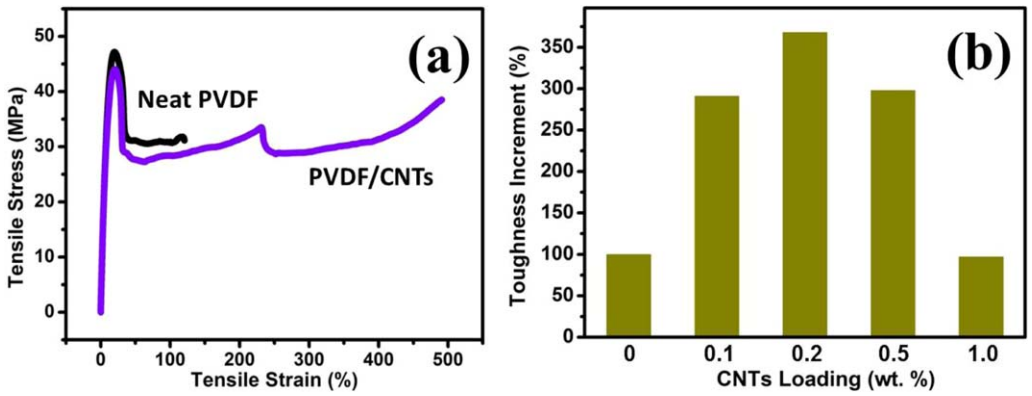

Figure 2. (a) Typical tensile test curves of neat PVDF and PVDF/CNTs composite sample with 0.2 wt % CNTs and (b) tensile toughness increments of composites normalized to that of neat PVDF. [Color figure can be viewed in the online issue, which is available at wileyonlinelibrary.com.]

processes employed for neat PVDF and PVDF composite samples were the same, the possibility of solvent plasticizing effect is eliminated. TEM image that shows the morphology of composite sample after tensile test (Supporting Information Figure S2a) reveals that most of the CNTs are not de-bonded from PVDF matrix. In addition, FESEM images of cryo-fractured

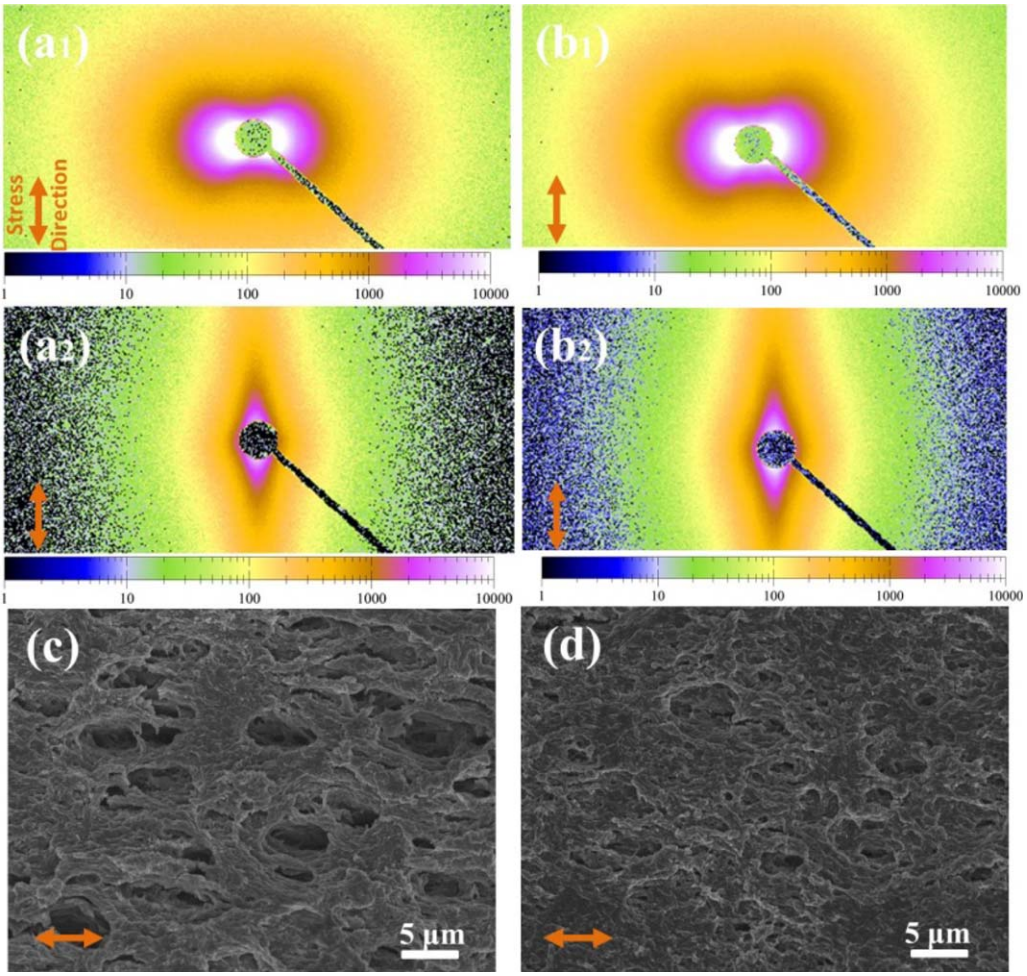

Figure 3. USAXS scattering patterns of (a1) neat PVDF, 30% strain; (b1) composite sample with 0.2 wt % CNTs, 30% strain; (a2) neat PVDF, 60% strain; (b2) composite sample with 0.2 wt % CNTs, 150% strain and FESEM of necking section of (c) neat PVDF and (d) composite sample with 0.2 wt % CNTs. To enable a clearer observation of morphological profile, both neat PVDF and composite sample are etched in oxidative solution of P_2O_5/H_2SO_4 before SEM. The arrows indicate the uniaxial stretching direction. [Color figure can be viewed in the online issue, which is available at wileyonlinelibrary.com.]

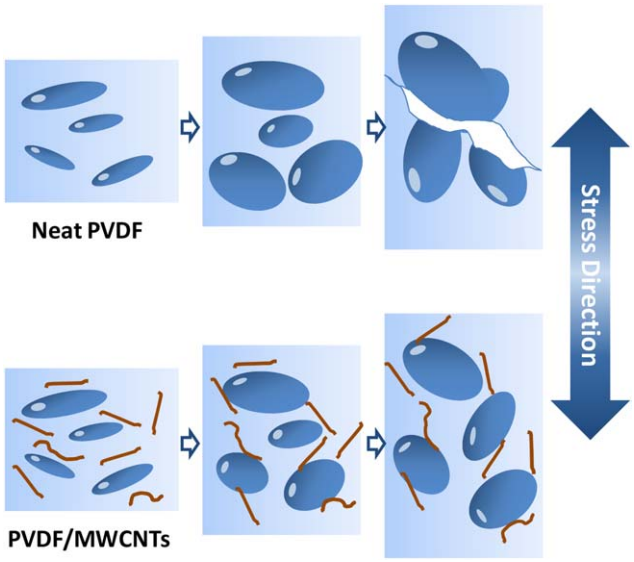

Figure 4. Illustration of the proposed mechanism of CNT pinning effect. The breakage of neat PVDF is caused by void development and coalescence under stress, while the realigned CNTs in PVDF/CNTs composite pin and impede the coalescence of voids, delaying the failure. [Color figure can be viewed in the online issue, which is available at wileyonlinelibrary.com.]

surface of tensile deformed sample in the transverse direction (Supporting Information Figure S2b) shows that even after stretching, the polymer matrix is still well coated on the surface of CNTs, further eliminating debonding as the factor. A previously reported simulation study on CNTs reinforced polymers stated that the stress-strain curve can be very sensitive to any debonding process and its occurrence would lead to a stress downturn or strain softening.[20] However, no such strain softening was observed in our tensile testing results, which again eliminates the possibility of debonding induced ductility.

Aravind *et al.*[19] prepared thermoplastic polypropylene with incubated pre-existent submicrometer voids and found that the voids growth resulted in the formation of energy-absorbing crazes, which could delay the fracture of polymer. In order to fully understand the effect of voids toward the mechanical properties of the PVDF/CNTs composites during stretching, *in-situ* USAXS analysis was carried out and the results are shown in Figure 3. It is seen that both neat PVDF and PVDF/CNTs composites possess abundant micrometer sized voids after tensile deformation, evidenced by the strong X-ray scattering intensity. This indicates that the exceptional ductility in our PVDF/CNT composite, which was not observed in neat PVDF, is not directly contributed by voids. In fact, as discussed earlier, CNTs debonding from the PVDF matrix after deformation is rarely seen, indicating negligible influence from debonding promoted voids formation, even if it takes place. In other words, CNTs do not cause the formation of voids in this study. It was also observed that when the deformation is small [Figure 3(a1,b1)], microvoids in both samples align along the direction that is vertical to the stress direction. As the deformation increases [Figure 3(a2,b2)], voids switched into the direction parallel to the stress for both neat PVDF and PVDF/CNT composites. Generally, microvoids are created with tips in the direction vertical to stress and develop along the stress direction. Despite the plenty of voids which are present in both neat PVDF and PVDF/CNT composite, we observed an obvious difference in the morphologies of necking section of the two deformed samples. It is seen that, from Figure 3(c,d), the void size of neat PVDF is noticeably larger than that of PVDF/CNT composite. The size of the voids in neat PVDF are around 5 μm, while that of composite sample is several times smaller ($1-2$ μm).

The void growth behavior observed in both USAXS and SEM analysis suggest the role of CNTs in improving the ductility and toughness of PVDF composites via delaying the voids coalescence. The introduction of CNTs may hinder the development of voids, delaying them from further growth. Consequently, before the breakage, PVDF/CNT composites could absorb more energy, corresponding to enhanced ductility, and tensile toughness. The difference in void growth found in neat PVDF and PVDF/CNTs composites is illustrated in Figure 4. For stretching of neat PVDF, perpendicular microvoids grow and realign towards the direction parallel to the stress direction [Figure 4, corresponding to the transition from Figure 3(a1,a2)]. Since there is no restriction, the propagating microvoids eventually coalesce with neighboring voids, forming larger voids and resulting in final failure. In the case of PVDF/CNT composites, CNTs in the path of crack propagation can pin and impede the growth, which slow down the coalescence of microvoids. After the initial propagating microvoids encounter CNTs, the fusion of neighboring voids is hindered. At the same time, more CNTs may realign parallel to the stress direction and becoming more effective in hindering voids growth. As a result, the formation and growth of voids will be delayed, hence leading to enhanced ductility and toughness.

Apart from void pinning effect of CNTs, the complex polymorphs of PVDF with different crystalline structures have to be considered. Owing to the substantial difference in modulus and ductility among each crystalline phases, any variations in the ratio of PVDF crystal structures is expected to exert considerable influence on physical properties of PVDF composites.[21,22] There are altogether five forms of chain arrangements of PVDF, among which, α, β, and γ phases are the most frequently observed and studied. α phase is the most thermodynamically stable phase and with a chain conformation of TGTG' (trans-gauche-trans-gauche); β phase has a chain conformation of TTTT (all trans) that is the main origin of the piezoelectric properties.[23] For γ phase, it has a chain sequence of TTTGTTTG' and is the transition state between α and β phases.[24] To investigate the effects of PVDF polymorphs on enhanced ductility, ATR-FTIR, XRD, and DSC were carried out to understand the polymorphic transformation during the tensile stretching process.

Figure 5(a,b) shows the DSC curves of neat PVDF and its composites before and after tensile testing, respectively. Two peaks are found in the DSC curve of neat PVDF before deformation. The weak endotherm peak at lower temperature of 148 °C is due to imperfect crystals formed in the process of melt crystallization.[25] The endotherm peak at 161 °C is attributed to α phase melting. For composite samples at all CNT loadings, a new shoulder peak at higher temperature of 167 °C emerged, which is the melting peak of γ phase PVDF. As summarized in Table II

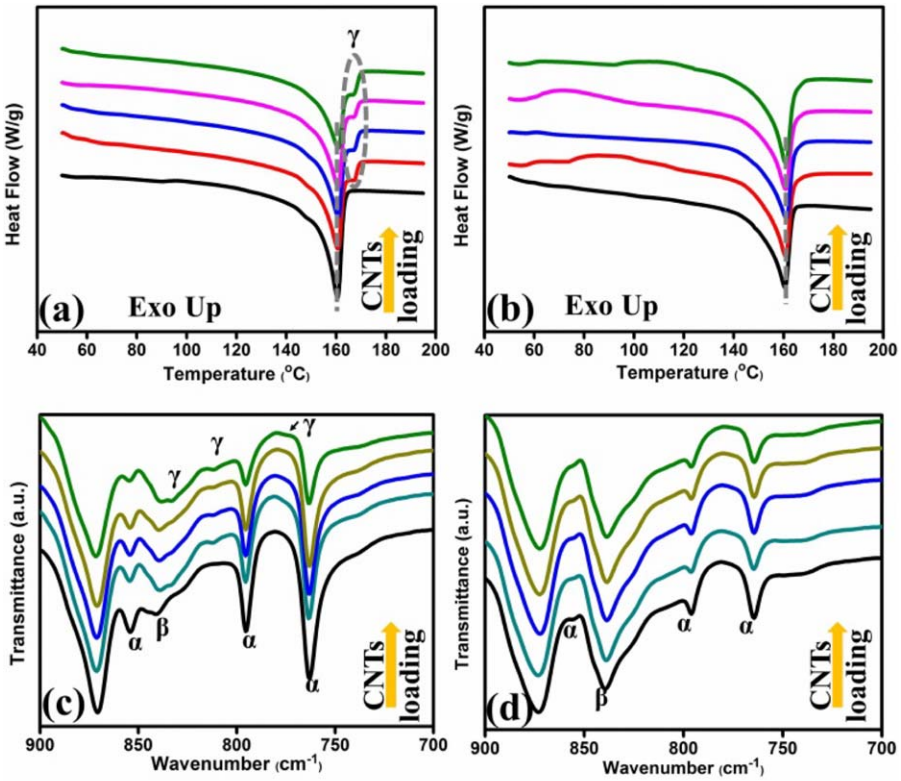

Figure 5. First heating DSC curves of PVDF/CNTs composites before (a) and after (b) tensile test and FTIR spectrum of PVDF/CNTs composites before (c) and after (d) tensile test. Curves from the bottom to top are spectrum of samples with 0, 0.1, 0.2, 0.5 and 1.0 wt % CNT, respectively. [Color figure can be viewed in the online issue, which is available at wileyonlinelibrary.com.]

are the melting points of each phase and the crystallinities of neat PVDF and composites, as obtained from DSC curves. Crystallinity was calculated by integrating the heat flow between 130 and 175 °C. The melting temperature of α phase barely alters with the increase of CNT loading, and is unaffected by tensile stretching. Melting temperature of γ crystallite remains comparable at different CNT contents. The crystallinities of as prepared PVDF composites, regardless of the different phases, decrease with the introduction of CNTs. However, the variations are very marginal. For example, the crystallinity of composite sample with 0.2 wt % CNTs is only 0.5% less than that of neat PVDF. The slightly reduced crystallinity could be partially responsible for the moderate change of modulus of composites. Furthermore, since γ crystallites possess much lower elastic modulus than that of α and β phase,[26] the existence of γ phase in composites may also affect the modulus. It is also seen from Figure 5(b) that the γ phase melting peak disappears after stretching, indicating the transformation into other phases.

FTIR is a useful tool that is frequently employed to differentiate each type of crystal in PVDF. Figure 5(c) shows the ATR-FTIR spectra of as-prepared neat PVDF and the corresponding CNT composites. FTIR peaks at 855, 796, and 764 cm^{-1} belonging to α crystallite are clearly seen in the spectra of both neat PVDF and composites. With the increase of CNTs loading, absorption of α crystallite decreases gradually, indicating decreased α phase in the composites. There is one peak at 840 cm^{-1} with weak intensity observed in FTIR spectra for both PVDF and CNT composites. Since both β and γ phases may absorb at this

Table II. Summary of the melting temperature and crystallinity of α and γ PVDF before and after stretching, as determined by DSC

CNT content (wt %)		0	0.1	0.2	0.5	1.0
$T_m(\alpha/\beta)$ (°C)	Before stretching	160.6	160.7	160.9	160.9	160.9
	After stretching	160.7	160.9	161.1	160.9	160.9
$T_m(\gamma)$ (°C)	Before stretching	-	167.5	167.3	167.3	167.1
	After stretching	-	-	-	-	-
Crystallinity	Before stretching	34.0	33.0	33.5	33.2	32.5
	After stretching	34.7	36.6	35.6	34.7	38.8

Enthalpy was calculated by integrating the heat flow between 130 and 175 °C by TA Analysis software and the fusion heat of 100% crystallinity is 102.5 J/g.[34]

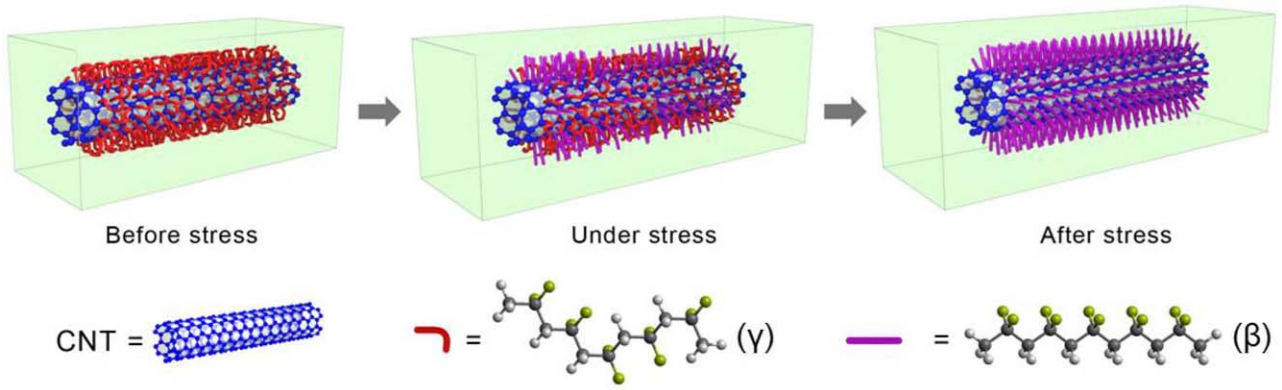

Figure 6. Illustration of the proposed mechanism of polymorphic transformation-induced ductility. Under stress, the γ phase in PVDF/CNTs composite around CNTs transform into β phase, creating plasticization and resulting in enhanced ductility and toughness. [Color figure can be viewed in the online issue, which is available at wileyonlinelibrary.com.]

wavenumber range, the origin of this peak cannot be determined at this point without further information. However, it is clear that a new peak at 833 cm^{-1} that exclusively belongs to γ crystallite[27] emerged for the composite samples, which is absent in the spectrum of neat PVDF. Additionally, absorptions at 812 and 716 cm^{-1} also come from γ phase, although the peak at 716 cm^{-1} is relatively weak. The peak at 840 cm^{-1} is attributed to β crystallite and its absorption increases after CNTs were introduced [Figure 5(c)]. This is consistent with other works that reported increased β phase after addition of nanomaterials into PVDF, such as nanoclay[28,29] and various types of CNTs.[30,31] The zigzag surface of CNTs is believed to match well with all-trans configurations which are beneficial to β PVDF growth formation.[32] This is further supported by simulation[31] that showed all-T configurations (β phase) are more favorable to be adsorbed onto the surface of CNT compared with TGTG' configuration. Molecules of α configuration are able to transform into β PVDF with the help of external energy input, for example via simple sonication. Since the γ phase is a transitional structure between α to β crystallite, it is reasonable to deduce that a portion of molecules on CNTs remain in γ configuration in the process of α/β transformation. γ PVDF is known to be crystallizing in the vicinity of the melting α phase.[33] Contributed by the melt crystallization occurred during both the melt extrusion and hot press processes, γ phase PVDF would form in the composites.

From Figure 5(d), it can be seen that, after the tensile test, all the α PVDF peaks decrease while that of the β phase at 840 cm^{-1} increases markedly, owing to the α to β transformation induced by stretching.[35] It is also noted that all absorptions of γ phase at 840, 812, and 776 cm^{-1} disappear after the stretching, indicating transformation of γ phase during the tensile test, consistent with DSC results. The transformation of γ phase, which is only present in composites during stretching, was also evidenced by XRD (Supporting Information Figure S3). In another words, based on the high similarity in chain configurations between β and γ PVDF, the γ PVDF transforms into β phase during stretching, similar to what was reported previously.[36] A separate simulation study[37] demonstrated that the phase transformation can be achieved in the way of interchain slippage, particularly along the molecule chain at the interface. As schematically illustrated in Figure 6, the γ phase slips into β phase under external load, where continuous slippage and transformation of γ phase create a plasticized zone around the β/γ phase interface in the vicinity of CNTs. This 'phase transformation induced plasticization' leads to significant enhancement of ductility and absorbs large amount of energy during stretching.

The findings in this study show that CNT is not only able to reinforce polymeric matrix in terms of Young's modulus and tensile strength; it can also remarkably enhance the ductility of the PVDF composites. The function of CNTs in PVDF matrix is two-fold. Firstly, CNTs serve as sites for void pinning during the stretching process. Secondly, the introduction of CNTs creates an interfacial PVDF crystal γ phase between the nanotube surface and the matrix, which undergoes polymorphic transformation during stretching. The synergistic effect of void pinning and interfacial phase transformation leads to exceptional improved ductility and toughness in PVDF/CNTs composites.

CONCLUSIONS

In summary, exceptionally ductile PVDF/MWCNTs composites with excellent dispersion of raw CNT in PVDF matrix have been prepared via a facile method combining solution mixing and melt blending. The highly ductile PVDF/MWCNTs composites were achieved without compromising the yield strength and modulus. The mechanism of such unique and counterintuitive ductility change is systematically investigated using various characterization techniques. USAXS revealed that CNTs acts as void pinning sites that hinder the propagation of microvoids, preventing their further coalescence. Furthermore, the polymorphic transformation was found to be another main contributing factor. In our system, γ phase PVDF in as-prepared composite samples disappeared and transformed into β crystallite during the stretching, creating plasticized zone around CNTs. This plasticization led to significant increase of ductility and toughness of the resultant composites. These types of highly ductile

PVDF/CNT composite with exceptional toughness are believed to be able to find wide potential for engineering applications.

ACKNOWLEDGMENTS

Xuelong Chen acknowledges the scholarship from Nanyang Technological University. The authors thank the facility for analysis, characterization, testing and simulation (FACTS) lab where SEM and XRD were performed. We also thank Dr. Yaotao Wang and Mr. Peng Hu on the helps of USAXS and TEM. This work is partially supported by A-Star through the MIMO program.

REFERENCES

1. Balazs, A. C.; Emrick, T.; Russell, T. P. *Science* **2006**, *314*, 1107.
2. Ramakrishna, S.; Mayer, J.; Wintermantel, E.; Leong, K. W. *Compos. Sci. Technol.* **2001**, *61*, 1189.
3. Paul, D.; Robeson, L. *Polymer* **2008**, *49*, 3187.
4. Kepler, R.; Anderson, R. *J. Appl. Phys.* **1978**, *49*, 1232.
5. Koga, K.; Ohigashi, H. *J. Appl. Phys.* **1986**, *59*, 2142.
6. Lin, S.-C.; Coates, M.; Pearce, E. M.; Huang, P.-T.; EP Patent 0,947,556 (**2004**).
7. Khayet, M.; Chowdhury, G.; Matsuura, T. *AIChE J.* **2002**, *48*, 2833.
8. Cui, Z.; Drioli, E.; Lee, Y. M. *Prog. Polym. Sci.* **2014**, *39*, 164.
9. Spitalsky, Z.; Tasis, D.; Papagelis, K.; Galiotis, C. *Prog. Polym. Sci.* **2010**, *35*, 357.
10. Mandal, A.; Nandi, A. K. *J. Mater. Chem.* **2011**, *21*, 15752.
11. Huang, W.; Edenzon, K.; Fernandez, L.; Razmpour, S.; Woodburn, J.; Cebe, P. *J. Appl. Polym. Sci.* **2010**, *115*, 3238.
12. Tang, X. G.; Hou, M.; Zou, J.; Truss, R.; Yang, M.; Zhu, Z. *Compos. Sci. Technol.* **2012**, *72*, 263.
13. Chang, C. M.; Liu, Y. L. *Carbon* **2010**, *48*, 1289.
14. Blake, R.; Coleman, J. N.; Byrne, M. T.; McCarthy, J. E.; Perova, T. S.; Blau, W. J.; Fonseca, A.; Nagy, J. B.; Gun'ko, Y. K. *J. Mater. Chem.* **2006**, *16*, 4206.
15. Kim, K. H.; Jo, W. H. *Compos. Sci. Technol.* **2008**, *68*, 2120.
16. Kim, K. H.; Jo, W. H. *Carbon* **2009**, *47*, 1126.
17. Notta-Cuvier, D.; Murariu, M.; Odent, J.; Delille, R.; Bouzouita, A.; Raquez, J. M.; Lauro, F.; Dubois, P. *Macromol. Mater. Eng.* **2015**, *300*, 684.
18. Ma, P.; Spoelstra, A.; Schmit, P.; Lemstra, P. *Eur. Polym. J.* **2013**, *49*, 1523.
19. Dasari, A.; Zhang, Q. X.; Yu, Z. Z.; Mai, Y. W. *Macromolecules* **2010**, *43*, 5734.
20. Needleman, A.; Borders, T.; Brinson, L.; Flores, V.; Schadler, L. *Compos. Sci. Technol.* **2010**, *70*, 2207.
21. Pei, Y.; Zeng, X. C. *J. Appl. Phys.* **2011**, *109*, 093514.
22. Corradini, P.; Guerra, G. In Macromolecules: Synthesis, Order and Advanced Properties; Springer, **1992**, *183*.
23. Ke, K.; Wang, Y.; Zhang, K.; Luo, Y.; Yang, W.; Xie, B. H.; Yang, M. B. *J. Appl. Polym. Sci.* **2012**, *125*, E49.
24. Jin, L.; Bower, C.; Zhou, O. *Appl. Phys. Lett.* **1998**, *73*, 1197.
25. Ince-Gunduz, B. S.; Alpern, R.; Amare, D.; Crawford, J.; Dolan, B.; Jones, S.; Kobylarz, R.; Reveley, M.; Cebe, P. *Polymer* **2010**, *51*, 1485.
26. Pei, Y.; Zeng, X. C. *J. Appl. Phys.* **2011**, 109.
27. Gregorio, R. *J. Appl. Polym. Sci.* **2006**, *100*, 3272.
28. Priya, L.; Jog, J. *J. Appl. Polym. Sci.* **2003**, *89*, 2036.
29. Patro, T. U.; Mhalgi, M. V.; Khakhar, D.; Misra, A. *Polymer* **2008**, *49*, 3486.
30. Levi, N.; Czerw, R.; Xing, S.; Iyer, P.; Carroll, D. L. *Nano Lett.* **2004**, *4*, 1267.
31. Yu, S.; Zheng, W.; Yu, W.; Zhang, Y.; Jiang, Q.; Zhao, Z. *Macromolecules* **2009**, *42*, 8870.
32. Manna, S.; Nandi, A. K. *J. Phys. Chem. C* **2007**, *111*, 14670.
33. Lovinger, A. J. *Polymer* **1980**, *21*, 1317.
34. Mead, W.; Zachariades, A. E.; Shimada, T.; Porter, R. S. *Macromolecules* **1979**, *12*, 473.
35. El Mohajir, B. E.; Heymans, N. *Polymer* **2001**, *42*, 5661.
36. Tashiro, K., Ed. Crystal Structure and Phase Transition of PVDF and Related Copolymers; New York: Marcel Dekker, **1995**.
37. Su, H.; Strachan, A.; Goddard, W. A. III, *Phys. Rev. B* **2004**, *70*, 064101.